Journal of Catalysis 263 (2009) 75–82

Contents lists available at ScienceDirect

Journal of Catalysis

www.elsevier.com/locate/jcat

Direct room-temperature synthesis of methyl-functionalized Ti-MCM-41 nanoparticles and their catalytic performance in epoxidation

Kaifeng Lin [a], Paolo P. Pescarmona [a,*], Kristof Houthoofd [a], Duoduo Liang [b], Gustaaf Van Tendeloo [b], Pierre A. Jacobs [a]

[a] COK, K.U. Leuven, Kasteelpark Arenberg 23-bus 2461, 3001 Heverlee, Belgium
[b] EMAT, UA, Groenenborglaan 171, 2020 Antwerpen, Belgium

ARTICLE INFO

Article history:
Received 8 July 2008
Revised 20 January 2009
Accepted 25 January 2009
Available online 13 February 2009

Keywords:
Methyl-functionalized Ti-MCM-41 nanoparticles
Dilute solution route
Shorter mesoporous channels
Epoxidation of cyclohexene
tert-Butyl hydroperoxide
Aqueous H_2O_2

ABSTRACT

Methyl-functionalized Ti-MCM-41 nanoparticles with a size of 80 to 160 nm (Me-Ti-MCM-41 NP) were directly prepared via a dilute solution route by the co-condensation of tetraethoxysilane and methylalkoxysilanes in sodium hydroxide medium at room temperature. The characterization results showed the existence of ordered hexagonal mesoporous structure and tetrahedral Ti species in the nanoparticles. In the epoxidation of cyclohexene with *tert*-butyl hydroperoxide and aqueous H_2O_2, Me-Ti-MCM-41 NP samples displayed higher turnover frequencies (TOFs) for cyclohexene and initial reaction rates compared to Ti-MCM-41 and methyl-functionalized Ti-MCM-41 with normal particle size and to non-functionalized Ti-MCM-41 nanoparticles. Simultaneously, a higher selectivity for cyclohexene epoxide was observed in the case of aqueous H_2O_2, suggesting that the hydrolysis of cyclohexene epoxide with water is reduced on Me-Ti-MCM-41 NP samples. The improved catalytic behavior of Me-Ti-MCM-41 NP is discussed both in terms of the nanosize and methylation of the surface of the catalyst particles. The regeneration of Me-Ti-MCM-41 NP with *tert*-butyl hydroperoxide solution was evaluated via washing and calcination approaches.

1. Introduction

Since the reported synthesis of microporous TS-1 [1], titanium-substituted zeolites have been attracting great attention because of their remarkable catalytic performance for selective oxidations of various organic substrates [2–8]. However, they cannot effectively catalyze conversion of bulky molecules, which have no access to the active sites located inside the micropores (0.7 nm). The discovery of ordered mesoporous titanosilicates with wider pore sizes (2–10 nm) [9–17] and mesoporous titanium-containing zeolite [18] overcomes this limitation and offers an opportunity to use titanosilicates as versatile catalysts in the oxidation of bulky reactant molecules. The most important features of the ordered mesoporous titanosilicates are the high surface area, which potentially allows an efficient dispersion of active sites, and the large and uniform pore diameters in the mesopore range, which favor the diffusion of bulky molecules. MCM-41, presenting a hexagonal array of unidirectional tubular pores, is one of the most studied ordered mesoporous structures [19]. Titanium-containing MCM-41 were reported for the first time in 1994 [9,10]. Since then Ti-MCM-41 materials have been studied as catalysts for various reactions, such as the epoxidation of olefins [10], unsaturated alcohols [20], plant oils [21], and the oxidation of organic sulfides [22]. In the oxidation of small reactant molecules, however, they show much lower catalytic activity than TS-1 and Ti-beta probably due to the lower hydrophobicity that promotes water adsorption, which poisons the catalytically active centers [11]. Ti-MCM-41 also suffers from leaching of the titanium active species in the presence of H_2O, which causes the gradual deactivation of the catalyst. Therefore, an enhancement of the hydrophobicity is considered important to improve the activity of Ti-MCM-41 and retard the Ti-leaching in liquid phase oxidation. Moreover, water removal from the catalyst surface would also reduce the hydrolysis of the epoxide product and, therefore, would be beneficial for the selectivity of the reaction. An increased hydrophobicity of the catalyst surface is also expected to favor the diffusion of the rather apolar alkene substrates inside the pores of the catalyst.

Two different successful approaches have been reported to enhance the surface hydrophobicity of Ti-MCM-41 by introducing organic groups into Ti-MCM-41 mesostructures. The first one involves postsynthetic silylation of the surface [23–26] and the second one is based on direct organic functionalization in one-step synthesis [27–32]. Both methods result in a remarkable enhancement of the catalytic activities in the epoxidation. However, in both cases, the synthesis step in which the mesoporous titanosilicate structure is formed includes a hydrothermal procedure that requires high temperature and pressure with the risk of formation

* Corresponding author. Fax: +32 16 321998.
E-mail address: paolo.pescarmona@biw.kuleuven.be (P.P. Pescarmona).

0021-9517/$ – see front matter
doi:10.1016/j.jcat.2009.01.013

of the anatase phase due to the high synthesis temperature. To our knowledge, no successful approach to directly prepare active organically-functionalized Ti-MCM-41 at room temperature in one step has been reported so far, although this would be an advantageous route compared with the hydrothermal procedure. A possible reason hindering this approach is the incomplete hydrolytic co-condensation of the different silicon and titanium sources at room temperature [32]. Additionally, it has been proposed that the large particle size of mesoporous titanosilicates is another major cause responsible for their reduced activity compared to Ti-substituted zeolites [30]. We recently prepared Ti-MCM-41 nanoparticles at room temperature, showing increased activity in the epoxidation of cyclohexene due to a decrease of particle size of Ti-MCM-41 into the nanoscale [33]. Therefore, the combination of introducing organic groups into Ti-MCM-41 mesostructures with the decrease in their particle size into the nanoscale is expected to create a mesoporous titanosilicate with improved catalytic performances.

In this article we describe the room-temperature synthesis of methyl-functionalized Ti-MCM-41 nanoparticles with short mesoporous channels and highly active titanium species. These materials were used to catalyze the epoxidation of cyclohexene with *tert*-butyl hydroperoxide and aqueous H_2O_2, which are frequently employed as test reactions for the catalytic evaluation of titanosilicate catalysts.

2. Experimental

2.1. Preparation of samples

Ti-MCM-41 nanoparticles (Ti-MCM-41 NP) were prepared from a dilute solution route as previously reported [33]. Methyl-functionalized Ti-MCM-41 nanoparticles were directly synthesized from the dilute solution route with a mixture of two silicon sources, tetraethyl orthosilicate (TEOS) and methyltriethoxysilane (MTES). First, 3.5 mL of 2 M NaOH aqueous solution was added to a stirred mixture of 480 mL of distilled water and 1.0 g of cetyltrimethylammonium bromide (CTAB). Secondly, titanium(IV) isopropoxide (TIP), TEOS and MTES were mixed into a solution at room temperature and then slowly added to the above-mentioned solution under stirring at 700–900 rpm, yielding a white gel with the following molar composition: 1197 H_2O/0.31 NaOH/0.125 CTAB/1 TEOS/*x*MTES/0.025 TIP, where *x* is 0.115 and 0.230. After stirring for 2 h at ambient temperature, the resulting solids were filtered, washed with 1500 mL of distilled water on a Büchner funnel, and dried at 60 °C. To remove the surfactant, the methyl-functionalized Ti-MCM-41 nanoparticles were treated with a solution of 1 M HCl in diethyl ether (solid:liquid = 1g:100 mL) for 24 h at room temperature. The solids were separated by centrifugation, washed with ethanol four times, and dried at 60 °C. The methyl-functionalized Ti-MCM-41 nanoparticles prepared by this route are denoted as 10% Me-Ti-MCM-41 NP and 19% Me-Ti-MCM-41 NP, where the percentage in the sample notation refers to the total amount of Me–Si in the starting gels. On the other hand, removal of the organics from the unfunctionalized Ti-MCM-41 samples was achieved by calcination in air at 550 °C for 6 h. All the samples were kept in capped plastic bottles (in air).

For comparison, Ti-MCM-41 and 19% Me-Ti-MCM-41 with conventional large particle size (designated as Ti-MCM-41 LP and 19% Me-Ti-MCM-41) were respectively synthesized using previously reported procedures [26,27,33].

2.2. Characterization

X-ray diffraction (XRD) patterns were obtained with a STOE STADI P instrument using Cu$K\alpha$ radiation. UV–visible spectra were measured with a Varian Cary 5 spectrophotometer equipped with a diffuse-reflectance accessory in the 200–800 nm region. In general, the samples were not treated before measurement and the UV–visible spectra were recorded in air. Selected samples were recorded also after in situ treatment in a U tube for 12 h at 350 °C in N_2. The isotherms of nitrogen were measured at liquid nitrogen temperature using a Micromeritics TriStar 3000. The pore-size distribution was calculated using the Barrett–Joyner–Halenda (BJH) model. Scanning electron microscopy (SEM) and transition electron microscopy (TEM) images were taken on a Philips XL30 FEG apparatus and a Philips CM 20 electron microscope, respectively. Si/Ti molar ratios and the presence of sodium in every sample were monitored by means of EDX analysis on a Philips XL30 FEG; every sample was measured three times and the average of the results was calculated. The ^{29}Si MAS NMR spectra were recorded on a Bruker AMX300 spectrometer (7.0 T). The spinning frequency of the rotor was 5000 Hz. Tetramethylsilane (TMS) was used as shift reference. FT-IR spectra of Me-Ti-MCM-41 NP before the first catalytic run and of the recycled sample after mild calcination were recorded on a Nicolet 730 FT-IR spectrometer using self-supported wafers of 6.7 mg/cm^2. The Si–CH_3 group is recognized by a band at ca. 1260 cm^{-1} [23]. Thermogravimetric analysis (TGA) was carried out under N_2 at a ramp of 10 °C/min with a TGA Q500 of TA instruments equipped with a high-throughput sampling platform designed for 16 samples.

The hydrophobicity of the samples was evaluated from TGA measurements of adsorbed water. The samples were pretreated in a desiccator in the presence of a saturated NH_4Cl solution for 72 h to reach the maximum level of water adsorption. The number of water molecules adsorbed on the surface of each sample was calculated from the weight loss between 25 and 150 °C measured by TGA, using the following equation

$$W = \frac{\Delta m}{M_{H_2O}} \frac{1}{A_{BET} m_i} N_A,$$

where W is the number of adsorbed H_2O molecules per nm^2; Δm is the weight loss in grams at a given temperature (g); m_i is the initial weight of the sample (g); M_{H_2O} is the molar mass of water (18.0153 g mol^{-1}); N_A is the Avogadro constant (6.022×10^{23} mol^{-1}); A_{BET} is the surface area (nm^2 g^{-1}) [34].

2.3. Catalytic reactions

The epoxidation of cyclohexene with *tert*-butyl hydroperoxide (TBHP) was carried out in a glass vial under vigorous stirring. In a typical run, 4.5 mmol of cyclohexene, TBHP (2.25 mmol, ~5.5 M in decane) and 30 mg of catalyst were mixed in the vial and heated to the desired temperature (35, 45, or 60 °C). After reaction, 4.5 mL of tetrahydrofuran was added to the reaction solution. The catalysts were separated by centrifugation and the products were analyzed on an Interscience Finnigan Trace GC Ultra equipped with a RTX-5 fused silica column (5 m, 0.1 mm). The TBHP efficiency was calculated as the ratio between the moles of TBHP used to form the epoxide and the moles of TBHP converted to ^{t}BuOH during the reaction [TBHP efficiency = ($mol_{epoxide}/mol_{BuOH}$) × 100%]. When aqueous H_2O_2 was used as an oxidant, the epoxidation of cyclohexene was carried out at 60 °C. 4.5 mmol of cyclohexene, 4.5 mL of acetonitrile, aqueous H_2O_2 (2.25 mmol, 50%) and 30 mg of catalyst were mixed in the vial. Each methylated Ti-MCM-41 NP catalyst was tested three times (each run on a fresh sample): averages of conversions and of turnover frequencies (TOF) are reported.

To prepare TBHP in dichloromethane (DCM), required amounts of TBHP (70% in water) were extracted into DCM using a separation funnel. The water layer was removed and the recovered organic layer was dried over 0.4 nm molecular sieves. The prepared TBHP in DCM was stored in a refrigerator until use.

For the recycling of the catalysts, the reaction solution was removed from each sample and 5 mL of ethanol was added to each vial. After stirring for 10 min, the solids were settled by centrifugation. Then, the supernatant ethanol solution was removed. The washing procedure was repeated 4 times. Finally, the samples were dried in an oven at 60 °C for 16 h.

3. Results and discussion

3.1. X-ray diffraction and nitrogen adsorption/desorption isotherms

The XRD patterns of Ti-MCM-41 NP and Me-Ti-MCM-41 NP samples exhibit reflections corresponding to the (100), (110) and (200) planes, indicating an ordered 2*d*-hexagonal (*p*6*mm*) arrangement of channels (Fig. 1). Comparing the values of d_{100} of as-synthesized Ti-MCM-41 NP, 10% Me-Ti-MCM-41 NP, and 19% Me-Ti-MCM-41 NP at 4.3, 4.2, and 4.0 nm, respectively, it follows that the unit cell size slightly decreases as the number of methyl groups increase.

N_2 adsorption/desorption isotherms of calcined Ti-MCM-41 NP, calcined Ti-MCM-41 LP, and Me-Ti-MCM-41 NP samples all give typical type-IV isotherms with a sharp inflection at $p/p_0 > 0.3$ (Fig. 2). This is characteristic of capillary condensation, which points to the uniformity of the mesopore size distribution. Table 1 lists textural properties of these samples. Calcined Ti-MCM-41 NP and Ti-MCM-41 LP present similar pore sizes and pore volumes. Considering the functionalized materials, 19% Me-Ti-MCM-41 NP exhibits slightly smaller pore size than 10% Me-Ti-MCM-41 NP, which can be attributed to the higher amount of methyl groups of the former. It is worth noting that the BET surface areas of Ti-MCM-41 NP and Me-Ti-MCM-41 NP samples from the dilute solution route are higher than of Ti-MCM-41 LP. This is mainly attributed to the smaller particle sizes of Ti-MCM-41 NP and Me-Ti-MCM-41 NP samples.

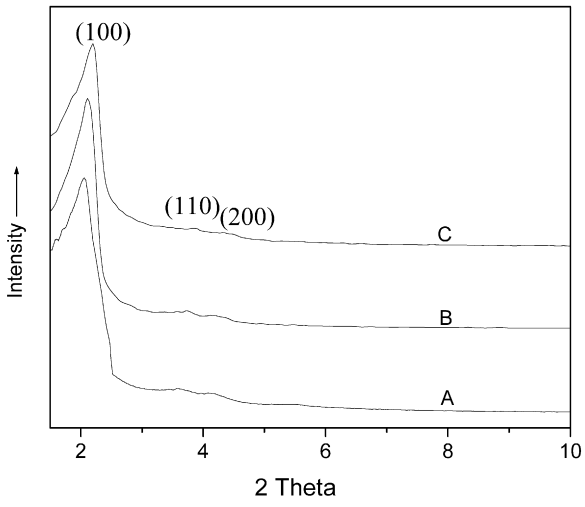

Fig. 1. X-ray diffraction pattern of Ti-MCM-41 NP (A), 10% Me-Ti-MCM-41 NP (B) and 19% Me-Ti-MCM-41 NP (C).

3.2. SEM and TEM images and EDX elemental analysis

The morphology and structure of Ti-MCM-41 NP and Me-Ti-MCM-41 NP samples are clearly revealed by SEM and TEM images. Ti-MCM-41 LP and 19% Me-Ti-MCM-41 consist of irregular agglomerated particles (Figs. 3A and 3B). In contrast, SEM images of Ti-MCM-41 NP and 10 and 19% Me-Ti-MCM-41 NP samples from the dilute solution route (Figs. 3C–3E) show nanosized spherulitic particles. The size of the particles ranges from 80 to 160 nm. TEM images of Ti-MCM-41 NP [33] and 10 and 19% Me-Ti-MCM-41 NP samples (Figs. 3F and 3G) show the existence of ordered hexagonal arrays and one-dimensional mesoporous parallel channels within these nanoparticles. The TEM results confirm that the Ti-MCM-41 nanoparticles are pure phases with short and ordered mesoporous channels. Although the synthesis was carried out in a Na-rich solution, negligible amounts of Na were incorporated in Ti-MCM-41 NP and Me-Ti-MCM-41 NP, as proven by EDX analysis.

In previous studies, it has been reported that the synthesis at room temperature for 3 days without hydrothermal treatment re-

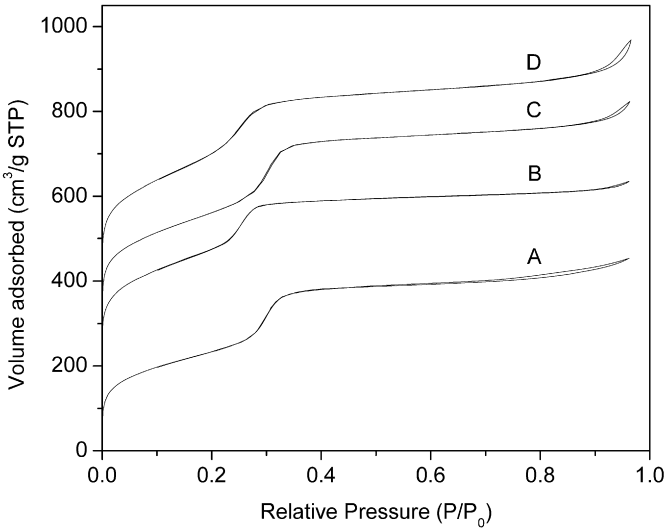

Fig. 2. N_2 adsorption/desorption isotherms of Ti-MCM-41 LP (A), Ti-MCM-41 NP (B), 10% Me-Ti-MCM-41 NP (C), and 19% Me-Ti-MCM-41 NP (D). For sake of clarity, spectra B, C and D are offset along the vertical axis by 200, 300 and 400 cm^3/g, respectively.

Table 1
Chemical composition, textural and structural properties.

	d_{100} (nm)	Pore size[a] (nm)	Pore volume[a] (cm^3/g)	Average particle size (nm)[e]	Surface area (m^2/g)	Methyl-group content[d] (mol%)	SiOH content[d] (mol%)	Si/Ti[b]
Ti-MCM-41 LP	3.8	2.1	0.54	–	847	–	42.8	47.4
Ti-MCM-41 NP	3.5	2.0	0.58	154	1013	–	42.3	129.1
10% Me-Ti-MCM-41 NP	4.2	2.3	0.62	135	1065	6.4	54.4	99.1
19% Me-Ti-MCM-41 NP	4.0	2.0	0.61	117	1323	12.1	45.0	94.7
19% Me-Ti-MCM-41	–	–	–	–	–	11.2	55.5	76.8
Uncalcined Ti-MCM-41 NP	4.3	–	–	–	–	–	56.7	–
Ti-MCM-41-20Me-0[c]	–	–	–	–	–	8.9	65.8	570

[a] Pore-size distributions and pore volumes derived from N_2 adsorption isotherms at 77 K.
[b] Molar ratios measured by EDX.
[c] From Ref. [32].
[d] Calculated from ^{29}Si MAS NMR spectra.
[e] Estimated from 50 randomly selected particles.

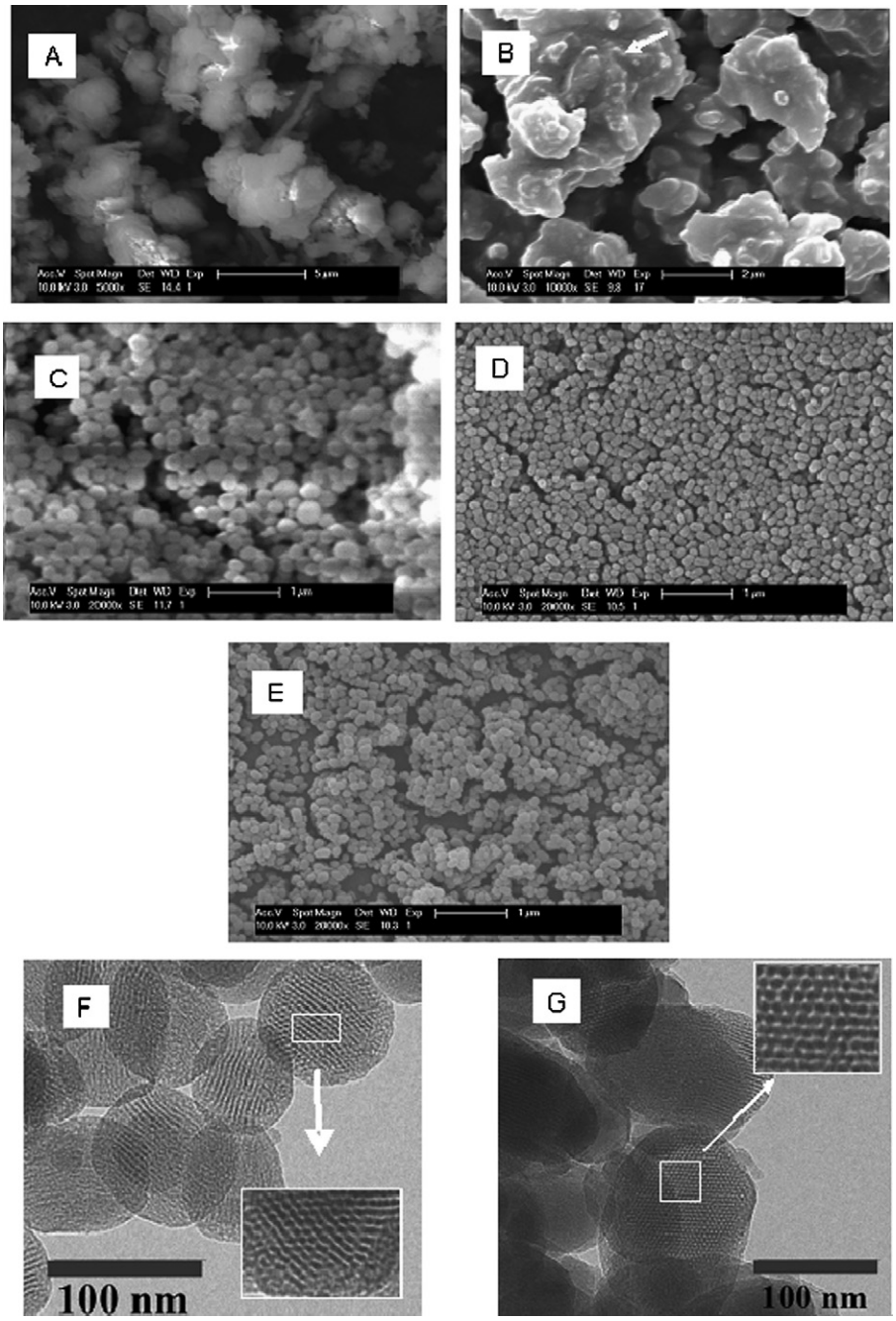

Fig. 3. SEM images of Ti-MCM-41 LP (A), 19% Me-Ti-MCM-41 (B), Ti-MCM-41 NP (C), 10% Me-Ti-MCM-41 NP (D), and 19% Me-Ti-MCM-41 NP (E) and TEM images of 10% Me-Ti-MCM-41 NP (F) and 19% Me-Ti-MCM-41 NP (G).

sults in an extremely high Si/Ti ratio (570) in methyl-functionalized Ti-MCM-41 [32]. It was proposed that the co-condensation of Ti and Si sources did not proceed effectively at room temperature and therefore Ti species might be washed out from the silica network during the template-extraction procedure using aqueous HCl. This is considered to be one of main reasons limiting the synthesis of organically functionalized titanium-containing mesoporous silicates at room temperature. However, Me-Ti-MCM-41 NP samples give much lower Si/Ti molar ratio (99.1 and 94.7) than in the reported procedure [32], indicating that the dilute solution route facilitates the inclusion of Ti species into the silica matrix by the effective co-condensation of Ti source and Si sources at room temperature. This can be explained in terms of the parameters influencing the kinetics of hydrolytic condensation reactions, such as the nature and the concentration of the Ti and Si sources, the solvent (if any), the amount of H_2O and the pH of the synthesis mixture [36]. The dilute solution route reported here presents a lower pH (12 instead of 13) and a lower concentration of Si and Ti sources compared to the literature method.

3.3. UV–visible spectroscopy

Fig. 4 shows the UV–vis spectra of calcined Ti-MCM-41 LP and Ti-MCM-41 NP, 19% Me-Ti-MCM-41 and Me-Ti-MCM-41 NP samples. All the samples exhibit a band centered at 217–224 nm attributed to distorted tetrahedral Ti species in mesoporous titanosilicates [32,35]. This indicates that Ti species are successfully incorporated into the silica framework via the dilute solution route. The spectra of Ti-MCM-41 LP and Ti-MCM-41 NP present a shoulder band at around 290 nm that can be attributed to reversible

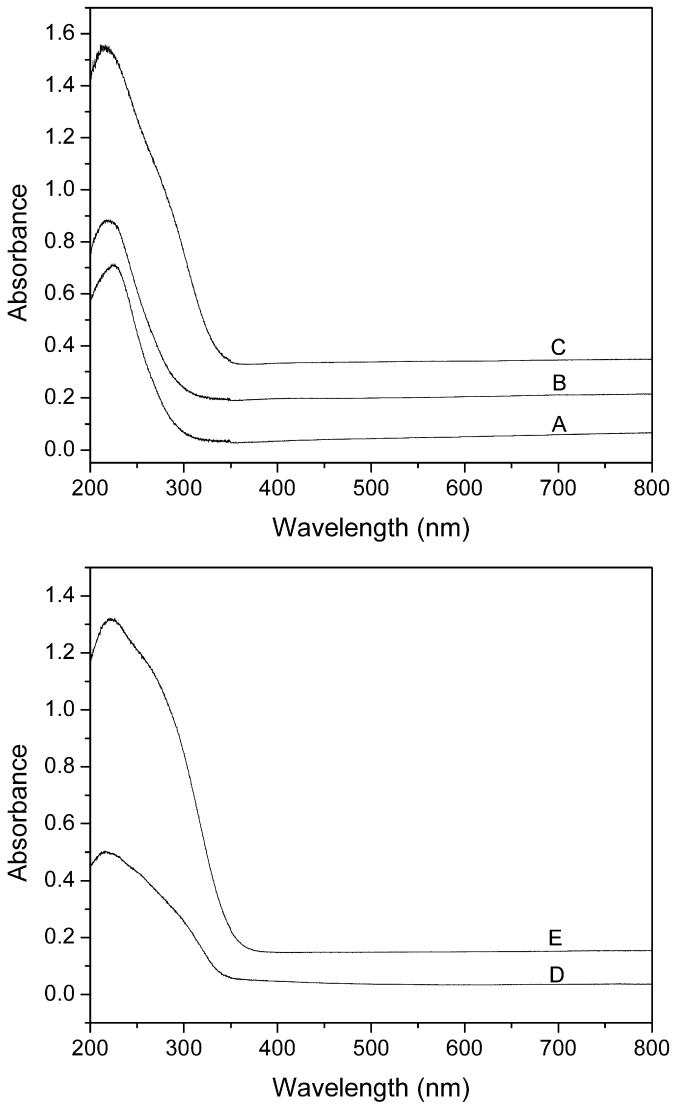

Fig. 4. UV–visible spectra of 10% Me-Ti-MCM-41 NP (A), 19% Me-Ti-MCM-41 NP (B), 19% Me-Ti-MCM-41 (C), Ti-MCM-41 NP (D), and Ti-MCM-41 LP (E). For sake of clarity, spectra B, C and E are offset along the vertical axis by 0.15, 0.3 and 0.1, respectively.

penta-coordinated Ti species forming from the interaction of Ti species with moisture and/or to polymerized hexa-coordinated Ti species [35]. Such a shoulder band is also visible but much less pronounced in the spectra of methyl-functionalized Ti-MCM-41 samples, indicating that these methylated materials have a larger fraction of Ti in tetrahedral sites. After in situ treatment at 350 °C for 12 h under N_2, the spectrum of anhydrous Ti-MCM-41 NP shows only a small shift of the shoulder band from 290 to 280 nm, indicating that this signal is due to irreversible species and, therefore, should be assigned to partially polymerized hexa-coordinated Ti species. The absence of a band at 330 nm indicates that anatase is absent in all samples.

3.4. ^{29}Si MAS NMR spectra and TGA

Fig. 5 shows the ^{29}Si MAS NMR spectra of various mesoporous titanosilicates. Ti-MCM-41 LP and Ti-MCM-41 NP exhibit three peaks at −110, −100, and −90 ppm, which are attributed to $(OSi)_4$ (Q^4), $HOSi(OSi)_3$ (Q^3), and $(HO)_2Si(OSi)_2$ (Q^2), respectively [26]. Methyl-functionalized Ti-MCM-41 nanoparticles show two extra peaks at −63 and −56 ppm, which are assigned to

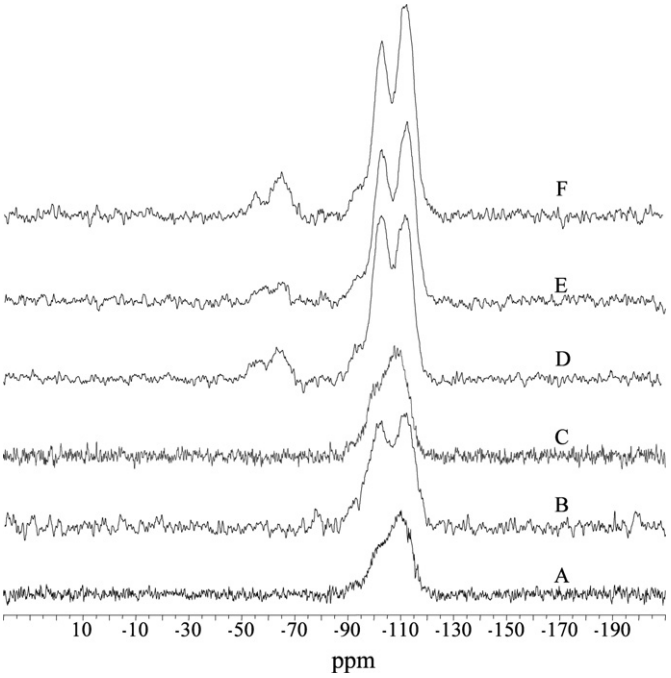

Fig. 5. ^{29}Si MAS NMR spectra of Ti-MCM-41 LP (A), uncalcined Ti-MCM-41 NP (B), Ti-MCM-41 NP (C), 19% Me-Ti-MCM-41 (D), 10% Me-Ti-MCM-41 NP (E), and 19% Me-Ti-MCM-41 NP (F).

$MeSi(OSi)_3$ (T^3) and $Me(HO)Si(OSi)_2$ (T^2). These results indicate that methyl groups can be incorporated well into the wall of Ti-MCM-41 NP by the direct synthesis from the dilute solution route. The organosiloxane incorporation, viz. methyl-group content, is determined by the following formula

$$\frac{100(T^2+T^3)}{\sum_i(Q^i+T^i)}\%$$

and given in Table 1.

Normally, the R-group content of the final material is greatly affected by hydrolysis rates of organosilanes at room temperature, since at low temperature the hydrolytic condensation rates of organosilicon species are rather low [32]. Some researchers observed that the hydrolytic condensation rates of alkylalkoxysilanes catalyzed by OH^- are lower than those of TEOS due to the electron-donating ability of alkyl groups bonded to Si (especially in the case of MTES) [32]. It has been reported that such a low hydrolytic condensation rate of MTES causes a much lower Me-content in methyl-functionalized Ti-MCM-41 than that in the starting gels. For instance, Ti-MCM-41 materials functionalized with methyl groups synthesized at room temperature were found to have Me-content of 8.9 mol% (mol%-MTES of total Si) from starting gels with a Me-content of 20 mol% [32]. The present Me-Ti-MCM-41 NP samples have Me-contents of 6 and 12 mol% from a Me-content of 10 and 19 mol% in the starting gels, respectively. This result suggests that the dilute solution route is a more effective method to incorporate methyl groups into the framework of Ti-MCM-41 by a direct organic functionalization at room temperature. This result can be explained with arguments similar to those used to discuss the improved incorporation of Ti species into the nanoparticles (see above). The synthesis of Me-Ti-MCM-41 NP occurs via a complex mechanism implying the hydrolysis and successive condensation of three different substances (TIP, TEOS, and MTES). The synthesis conditions used in this work seem to be more efficient than previously reported methods in promoting a concerted condensation of the Si and Ti sources at room temperature, leading to Ti-MCM-41 with higher Ti content and higher degree of functionalization.

Table 2
Catalytic performances in the epoxidation of cyclohexene with TBHP solution over various catalysts.[a]

	Si/Ti	Conv.[b] (%)	TBHP efficiency (%)	TOF (h^{-1})[c] (based on CH)	Selectivity for CHE (%)	TOF (h^{-1})[d] (based on CHE)
Ti-MCM-41 NP	129.1	16.3	89.5	38.3	88.2	33.8
Ti-MCM-41 LP	47.4	13.0	79.7	11.4	69.9	8.0
10% Me-Ti-MCM-41 NP	99.1	31.7	90.7	57.3	94.3	54.0
19% Me-Ti-MCM-41 NP	94.7	38.5	98.2	66.6	94.1	62.7
19% Me-Ti-MCM-41	76.8	43.7	> 99	61.5	95.8	58.9

[a] Reaction conditions: 4.5 mmol of cyclohexene, 2.25 mmol of TBHP (~5.5 M in decane), 30 mg of catalyst, 60 °C, 5 h.
[b] Based on cyclohexene.
[c] Turnover frequency is moles of cyclohexene converted per mole Ti active site of the catalyst per hour.
[d] Turnover frequency is moles of cyclohexene epoxide formed per mole Ti active site of the catalyst per hour.

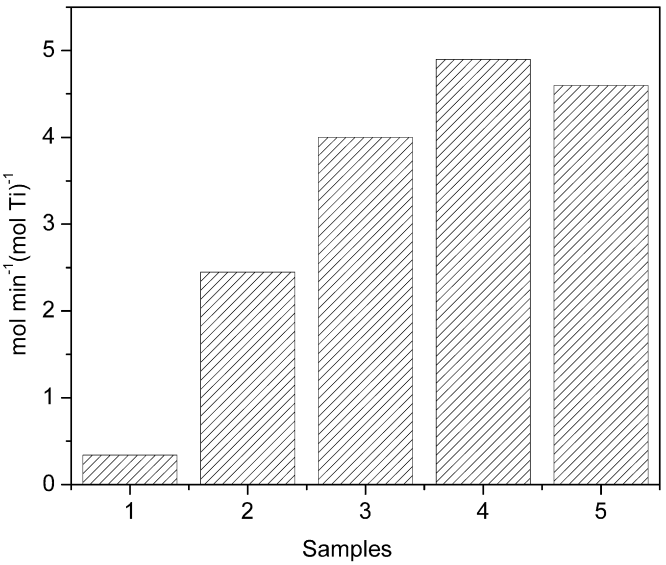

Fig. 6. Initial rate after 30 min of cyclohexene epoxidation based on cyclohexene epoxide over various catalysts with TBHP (~5.5 M in decane). Sample 1-5: Ti-MCM-41 LP, Ti-MCM-41 NP, 10% Me-Ti-MCM-41 NP, 19% Me-Ti-MCM-41 NP and 19% Me-Ti-MCM-41. For the reaction conditions, see Table 2.

The percentage of SiOH groups on all Si atoms (SiOH content) derived from the ^{29}Si MAS NMR analysis are listed in Table 1, which are calculated by the following equation

$$\frac{100(2Q^2 + Q^3 + T^2)}{\sum_i (Q^i + T^i)}\%.$$

The SiOH content of the samples decreases in the following order: uncalcined Ti-MCM-41 NP > 19% Me-Ti-MCM-41 > 10% Me-Ti-MCM-41 NP > 19% Me-Ti-MCM-41 NP > Ti-MCM-41 LP > Ti-MCM-41 NP. The lowest SiOH contents are observed in calcined Ti-MCM-41 NP and Ti-MCM-41 LP samples due to the condensation of SiOH groups upon calcination. For the other samples prepared at room temperature without calcination, Me-Ti-MCM-41 NP samples show lower SiOH content than uncalcined Ti-MCM-41 NP due to the incorporation of methyl groups in the framework.

The hydrophobicity of the Ti-MCM-41 NP samples was evaluated by TGA from the amount of adsorbed water, which is calculated from the weight loss of the samples between 25 and 150 °C. The number of adsorbed water molecules per nm^2 of Ti-MCM-41 NP, 10% Me-Ti-MCM-41 NP and 19% Me-Ti-MCM-41 NP is 3.1, 2.5 and 1.6, respectively, indicating that the hydrophobicity is enhanced by the incorporation of Me groups on the surface.

3.5. Catalytic results

Table 2 summarizes the catalytic activities of the inorganic and organically functionalized Ti-MCM-41 catalysts in the epoxidation of cyclohexene with TBHP (~5.5 M in decane) as an oxidant. With every catalyst tested, the main product in the epoxidation of cyclohexene was cyclohexene epoxide (CHE), with up to 96% selectivity. All the catalysts display high TBHP efficiency, with higher values (%) for higher epoxide yields. Among the studied catalysts, 19% Me-Ti-MCM-41 NP displayed the highest TOF values based on both cyclohexene and cyclohexene epoxide and the highest initial reaction rate calculated by the production of cyclohexene epoxide after 30 minutes of reaction (Fig. 6). The improved catalytic results obtained with this mesoporous titanosilicate are attributed to the combined advantages of incorporated methyl groups and nanosized particles of Ti-MCM-41: the comparatively higher hydrophobicity and shorter length of the mesoporous channels result in the enhanced diffusion of both cyclohexene and TBHP to the active Ti-sites. Ti-MCM-41 NP and 19% Me-Ti-MCM-41 NP displayed higher TOF values based on cyclohexene compared with the corresponding materials with larger particles, viz. Ti-MCM-41 LP and 19% Me-Ti-MCM-41. This is attributed to the decreased particle size of Ti-MCM-41 into nanometer scale, allowing an enhanced accessibility of the reactants to the catalytic Ti species in the shorter channels of Ti-MCM-41 NP and 19% Me-Ti-MCM-41 NP, which is in good agreement with previous work [33]. The improved diffusion in the shorter pore channels may also prevent clogging of the pores by heavy products that would cause deactivation of the catalysts. All the methyl-functionalized Ti-MCM-41 samples showed higher catalytic activities than the non-functionalized Ti-MCM-41 samples. This is ascribed not only to the improved hydrophobicity stemming from the methylation of the surface, but also to the larger fraction of Ti as catalytically active tetrahedral species in the methyl-functionalized samples (see Section 3.3). However, the difference in activity between 10% Me-Ti-MCM-41 NP and 19% Me-Ti-MCM-41 NP is attributed only to the effect of the hydrophobicity since the two methyl-functionalized samples present similar distribution of Ti species as proved by UV–vis spectroscopy.

Table 3
Catalytic performances in the epoxidation of cyclohexene in different TBHP solutions and solvents at different temperature over 10% Me-Ti-MCM-41 NP catalyst.[a]

Temperature (°C)	TBHP solutions	Solvent	Conv. (%)[b]	Selectivity for CHE (%)
60	~5.5 M in decane	–	31.7	94.3
60	~5.5 M in decane	3 mL of MeCN	31.0	90.2
60	~5.5 M in decane	3 mL of decane	16.3	88.1
35	~5.5 M in decane	–	14.9	78.6
35	~3 M in DCM	–	34.6	95.2
45	~5.5 M in decane	–	17.6	83.0

[a] Reaction conditions: 4.5 mmol of cyclohexene, 2.25 mmol of TBHP, 30 mg of catalyst, 5 h.
[b] Based on cyclohexene.

Table 3 lists the catalytic performances of 10% Me-Ti-MCM-41 NP in different TBHP solutions at different temperatures with/without co-solvents. When acetonitrile was used as a co-solvent at 60 °C, the catalytic activity and selectivity for CHE were similar as those when no co-solvent was used. However,

Table 4
Catalytic performances in the epoxidation of cyclohexene with aqueous H_2O_2 over various catalysts[a].

	Si/Ti (molar)	Conv. (%)[b]	TOF (h^{-1})[c] (based on CH)	Selectivity for CHE (%)	TOF (h^{-1})[d] (based on CHE)
Ti-MCM-41 NP	129.1	4.9	115.0	12.2	14.0
Ti-MCM-41 LP	47.4	5.7	50.0	10.3	5.2
10% Me-Ti-MCM-41 NP	99.1	8.4	151.9	13.4	20.3
19% Me-Ti-MCM-41 NP	94.7	8.9	153.8	14.0	21.5
19% Me-Ti-MCM-41	76.8	8.5	119.5	11.0	13.1

[a] Reaction conditions: 4.5 mL of MeCN, 4.5 mmol of cyclohexene, 2.25 mmol of H_2O_2 (50 wt% in water), 30 mg of catalyst, 60 °C, 0.5 h.
[b] Based on cyclohexene.
[c] Turnover frequency is moles of cyclohexene converted per mole Ti active site of the catalyst per hour.
[d] Turnover frequency is moles of cyclohexene epoxide formed per mole Ti active site of the catalyst per hour.

the activity decreased when additional decane was used, suggesting that a long linear alkane as decane can adsorb on the methyl-functionalized catalyst surface, thus retarding the contact of cyclohexene and TBHP with the titanium sites. To further evaluate the effect of solvents, a new TBHP solution (~3 M in DCM) was prepared and used as an oxidant. A much higher catalytic activity at 35 °C was detected with the new kind of TBHP solution than with TBHP in decane solution. These results confirm the detrimental effect of decane molecules on the catalytic activity in such reaction.

When aqueous H_2O_2 was used as an oxidant, four different products of the oxidation of cyclohexene were detected: cyclohexene epoxide (CHE), 1,2-cyclohexanediol (CHD), 2-cyclohexene-1-ol (CH–OH) and 2-cyclohexene-1-one (CH–ONE). It has been revealed that the O–O bond of Ti-oxo species (Ti-peroxo, Ti-hydroperoxo or Ti-superoxo) generated on titanosilicate molecular sieves by contact with H_2O_2 cleaves either heterolytically or homolytically. The heterolytic cleavage leads to the epoxide product (CHE), while the homolytic cleavage leads to the allylic oxidation products (CH–OH and CH–ONE) [37]. CHD is formed by catalytic hydrolysis of the epoxide ring of cyclohexene oxide in the presence of acid sites. Table 4 presents the catalytic performances of the inorganic and organically functionalized Ti-MCM-41 catalysts in the epoxidation of cyclohexene with aqueous H_2O_2 in acetonitrile. The conversion of cyclohexene in the presence of H_2O_2 with no catalyst and with Si-MCM-41 is 0.5 and 0.6%, respectively, indicating that the self-oxidation and/or radical oxidation play a minor role in the activity measured with the Ti-catalysts. Ti-MCM-41 NP and 19% Me-Ti-MCM-41 NP displayed higher TOF value and selectivity for CHE than Ti-MCM-41 LP and 19% Me-Ti-MCM-41, respectively. This result points to the advantages of the enhanced accessibility to the catalytic Ti species for the reactants and of the shorter residence time of CHE in the shorter channels of Ti-MCM-41 NP and 19% Me-Ti-MCM-41 NP samples, in agreement with earlier reports [33]. When compared with Ti-MCM-41 NP, Me-Ti-MCM-41 NP samples exhibited higher activities and selectivities for CHE. The higher selectivities are ascribed to a reduced hydrolysis of cyclohexene epoxide with H_2O: the enhanced surface hydrophobicity generated by the methylation (as estimated by TGA) favors the removal of H_2O formed from H_2O_2 during the epoxidation. The higher activities are attributed to the improved surface hydrophobicity favoring the access of cyclohexene to the active sites and reducing the poisoning effect of water, as well as to the larger fraction of Ti in the form of tetrahedral species in Me-Ti-MCM-41 NP, as mentioned before. The slightly higher activity displayed by 19% Me-Ti-MCM-41 NP compared with 10% Me-Ti-MCM-41 NP[1] is ascribed uniquely to the increase in hydrophobicity with the degree of methyl-functionalization, as discussed above for the epoxidation with TBHP.

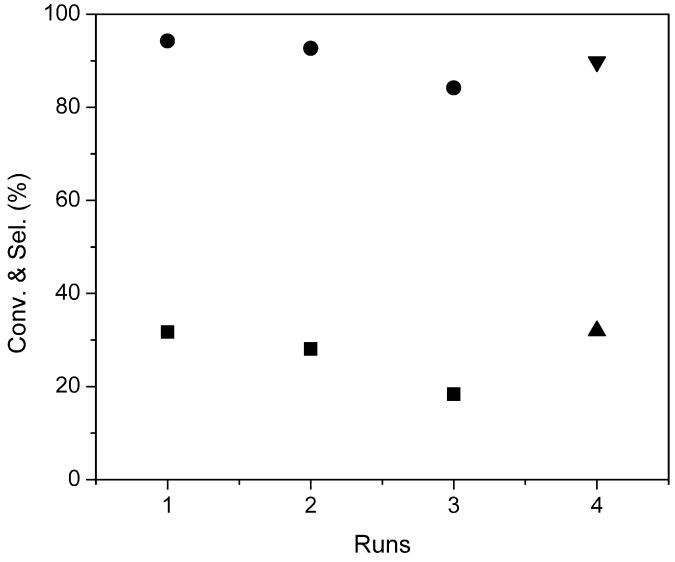

Fig. 7. Catalytic activity (■ and ▲) and selectivity for CHE (● and ▼) of repeated use of 10% Me-Ti-MCM-41 NP in the epoxidation of cyclohexene with TBHP (~5.5 M in decane) by washing (■ and ●) and mild calcination (▲ and ▼) approaches.

In order to evaluate the recyclability potential of the samples, 10% Me-Ti-MCM-41 NP was washed and reused in several 5-h catalytic cycles with TBHP solution (~5.5 M in decane). Fig. 7 shows the results of the repeated use of Ti-MCM-41 NP after four room temperature washings with ethanol (Runs 2 and 3) and calcination (Run 4). In the washing case, the cyclohexene conversion and selectivity for CHE gradually decreased during subsequent runs, probably to be attributed to the deposition of reaction residue around the catalytically active sites on the surface and/or the leaching of titanium during the reaction as observed for the classically prepared Ti-MCM-41. An alternative approach on regenerability of 10% Me-Ti-MCM-41 NP was via intermediate mild calcination at 300 °C for 2 h under N_2. Under these conditions, the methyl groups on the catalyst were mostly preserved, as indicated by the detection of the peaks due to the Si–CH_3 group [23] in the FT-IR spectra of the material both before the first catalytic run and after mild calcination. The almost complete reactivation of the used 10% Me-Ti-MCM-41 NP was achieved by this calcination procedure (Run 4), giving comparable conversion as that in Run 1. It can be concluded that the gradual decrease in cyclohexene conversion is due to heavy product deposition because adsorbed reaction residues that hinder the access of the reagents to the active centers would be removed during the intermediate calcination. However, the selectivity for CHE slightly decreases, which might be attributed to

[1] Given the small difference in activity and selectivity between 10% Me-Ti-MCM-41 NP and 19% Me-Ti-MCM-41 NP, each sample was tested three times (each run on a fresh sample) and the averages of activities were reported. In each run, 19% Me-Ti-MCM-41 NP displayed higher activity and selectivity than 10% Me-Ti-MCM-41 NP, proving that the difference in the reported values is meaningful, although small.

the aggregation of Ti-MCM-41 NP particles and/or the change of Ti coordinated environment from their original location during calcination.

4. Conclusions

Methylated Ti-MCM-41 nanoparticles (Me-Ti-MCM-41 NP) with highly active titanium species were prepared at room temperature from a dilute solution route. Characterization of these nanoparticles indicates the formation of ordered hexagonal arrays and one-dimensional mesoporous parallel channels and the incorporation of the methyl groups. The dilute solution route reported here not only is a successful method to prepare Ti-MCM-41 nanoparticles, but is also a more effective method to incorporate methyl groups into the framework of Ti-MCM-41 by a direct organic functionalization at room temperature.

In the epoxidation of cyclohexene with TBHP, 19% Me-Ti-MCM-41 NP showed the highest TOF and initial reaction rate among various mesoporous titanosilicates. When aqueous H_2O_2 was used as the oxidant, 19% Me-Ti-MCM-41 NP was again the best catalyst, displaying the highest TOF and selectivity based on cyclohexene epoxide.

The improved catalytic performance of 19% Me-Ti-MCM-41 NP is ascribed to a combined effect of its shorter mesoporous channels and of the improved hydrophobicity generated by the incorporation of the methyl groups.

The gradual decrease in cyclohexene conversion in the regeneration of the methyl-functionalized catalysts via washing approach is ascribed to heavy product deposition on the catalyst surface. The other possible regeneration approach is an intermediate mild calcination resulting in almost complete reactivation.

Acknowledgments

K.L. is grateful for a Center of Excellence grant (CECAT) from K.U. Leuven. P.P.P. acknowledges FWO for a postdoc grant. The authors acknowledge sponsoring in the frame of the following research programs: CECAT (K.U. Leuven, Flemish Government), SBO-BIPOM (IWT), IAP-PAI (BELSPO, Federal Government), NoE IDECAT (EU) and GOA (Flemish Government). We thank Gina Vanbutsele for assistance in the measurement of the N_2 isotherms.

References

[1] M. Taramasso, G. Perego, B. Notari, US Patent 4410501, 1983.
[2] A. Tuel, Zeolites 15 (1995) 236.
[3] D.P. Serrano, H.X. Li, M.E. Davis, Chem. Commun. (1992) 745.
[4] A. Corma, M.A. Camblor, P. Esteve, A. Martínez, J. Pérez-Pariente, J. Catal. 145 (1994) 151.
[5] T. Tatsumi, N. Jappar, J. Phys. Chem. B 102 (1998) 7126.
[6] A. Corma, P. Esteve, A. Martínez, J. Catal. 161 (1996) 11.
[7] B. Notari, Adv. Catal. 41 (1996) 253.
[8] P. Ratnasamy, D. Srinivas, H. Knözinger, Adv. Catal. 48 (2004) 1.
[9] P.T. Tanev, M. Chibwe, T.J. Pinnavaia, Nature 368 (1994) 321.
[10] A. Corma, M.T. Navarro, J. Pérez-Pariente, Chem. Commun. (1994) 147.
[11] T. Blasco, A. Corma, M.T. Navarro, J. Pérez-Pariente, J. Catal. 156 (1995) 65.
[12] K.A. Koyano, T. Tatsumi, Chem. Commun. (1996) 145.
[13] O. Franke, J. Rathousky, G. Schulz-Ekloff, J. Starek, A. Zukal, Stud. Surf. Sci. Catal. 84 (1994) 77.
[14] I.F. Vankelecom, N.M. Moens, K.A. Vercruysse, A.L. Karen, R.F. Parton, P.A. Jacobs, Stud. Surf. Sci. Catal. 108 (1997) 437.
[15] D.T. On, M.P. Kapoor, P.N. Joshi, L. Bonneviot, S. Kaliaguine, Catal. Lett. 44 (1997) 171.
[16] T. Maschmeyer, F. Rey, G. Sankar, J.M. Thomas, Nature 378 (1995) 159.
[17] K.A. Vercruysse, D.M. Klingeleers, T. Colling, P.A. Jacobs, Stud. Surf. Sci. Catal. 117 (1998) 469.
[18] I. Schmidt, A. Krogh, K. Wienberg, A. Carlsson, M. Brorson, C.J.H. Jacobsen, Chem. Commun. (2000) 2157.
[19] P. Selvam, S.K. Bhatia, C.G. Sonwane, Ind. Eng. Chem. Res. 40 (2001) 3237.
[20] C. Berlini, M. Guidotti, G. Moretti, R. Psaro, N. Ravasio, Catal. Today 60 (2000) 219.
[21] L.A. Rios, P. Weckes, H. Schuster, W.F. Hoelderich, J. Catal. 232 (2005) 19.
[22] A. Corma, M. Iglesias, F. Sanchez, Catal. Lett. 39 (1996) 153.
[23] J. Bu, H.-K. Rhee, Catal. Lett. 65 (2000) 141.
[24] M. Guidotti, I. Batonneau-Gener, E. Gianotti, L. Marchese, S. Mignard, R. Psaro, M. Sgobba, N. Ravasio, Microporous Mesoporous Mater. 111 (2008) 39.
[25] T. Tatsumi, K.A. Koyano, N. Igarashi, Chem. Commun. (1998) 325.
[26] K. Lin, L. Wang, F. Meng, Z. Sun, Q. Yang, Y. Cui, D. Jiang, F.-S. Xiao, J. Catal. 235 (2005) 423.
[27] A. Corma, J.L. Jordá, M.T. Navarro, F. Rey, Chem. Commun. (1998) 1899.
[28] N. Igarashi, S. Kidani, R. Ahemaito, T. Tatsumi, Stud. Surf. Sci. Catal. 129 (2000) 163.
[29] N. Igarashi, S. Kidani, R. Ahemaito, T. Tatsumi, Zeolitic Mater. 1 (2001) 15.
[30] A. Bhaumik, T. Tatsumi, J. Catal. 189 (2000) 31.
[31] A. Bhaumik, T. Tatsumi, Catal. Lett. 66 (2000) 181.
[32] N. Igarashi, S. Kidani, R. Ahemaito, K. Hashimoto, T. Tatsumi, Microporous Mesoporous Mater. 81 (2005) 97.
[33] K. Lin, P.P. Pescarmona, H. Vandepitte, D. Liang, G. Van Tendeloo, P.A. Jacobs, J. Catal. 254 (2008) 64.
[34] R. Rinaldi, U. Schuchardt, J. Catal. 227 (2004) 109.
[35] E. Gianotti, C. Bisio, L. Marchese, M. Guidotti, N. Ravasio, R. Psaro, S. Coluccia, J. Phys. Chem. C 111 (2007) 5083.
[36] P.P. Pescarmona, T. Maschmeyer, Aust. J. Chem. 54 (2001) 583.
[37] V.N. Shetti, D. Srinivas, P. Ratnasamy, Z. Phys. Chem. 219 (2005) 905.